Compliance of single frequency ionospheric delay estimation and cycle slip detection with Civil Aviation requirements

Christophe Ouzeau, Christophe Macabiau, Anne-Christine Escher, Benoit
Roturier

HAL Id: hal-01021984
https://enac.hal.science/hal-01021984

Submitted on 27 Oct 2014

Compliance of Single Frequency Ionospheric Delay Estimation and Cycle Slip Detection with Civil Aviation Requirements

Christophe Ouzeau, *ENAC/TéSA/DTI*
Christophe Macabiau, *ENAC*
Anne-Christine Escher, *ENAC*
Benoît Roturier, *DSNA-DTI*

BIOGRAPHY

Christophe OUZEAU graduated in 2005 with a master in astronomy at the Observatory of Paris. He started the same year his Ph.D. thesis on degraded modes resulting from the multiconstellation use of GNSS, supported by DTI and supervised by ENAC.

Christophe MACABIAU graduated as an electronics engineer in 1992 from the ENAC in Toulouse, France. Since 1994, he has been working on the application of satellite navigation techniques to civil aviation. He received his PhD in 1997 and has been in charge of the signal processing lab of the ENAC since 2000.

Anne-Christine ESCHER graduated as an electronics engineer in 1999 from the ENAC in Toulouse, France. Since 2002, she has been working as an associated researcher in the signal processing lab of the ENAC. She received her Ph.D. in 2003.

Benoît ROTURIER graduated as a CNS systems engineer from Ecole Nationale de l'Aviation Civile (ENAC), Toulouse in 1985 and obtained a PhD in Electronics from Institut National Polytechnique de Toulouse in 1995. He was successively in charge of Instrument Landing Systems at DGAC/STNA (Direction Générale de l'Aviation Civile/Service Technique de la Navigation Aérienne), then of research activities on CNS systems at ENAC. He is since 2000 head of GNSS Navigation subdivision at DGAC/DTI (Direction de la Technique et de l'Innovation, formerly known as STNA) and is involved in the development of civil aviation applications based on GPS/ABAS, EGNOS and GALILEO. He is also currently involved in standardization activities on future multiconstellation GNSS receivers within Eurocae WG62 and is the chairman of the technical group of ICAO Navigation Systems Panel.

ABSTRACT

Ionosphere is a dispersive medium that can strongly affect GPS and GALILEO signals. Ionospheric delay affecting the GPS and GALILEO single frequency pseudorange measurements is the largest source of ranging error. In addition, this perturbation is difficult to model and thus difficult to predict. Nominal dual frequency measurements provide a good estimation of ionospheric delay. In addition, the combination of GPS and GALILEO navigation signals at the receiver level is expected to provide important improvements for civil aviation. It could, potentially with augmentations, provide better accuracy and availability of ionospheric correction measurements. Indeed, GPS users will be able to combine GPS L1 and L5 frequencies, and future GALILEO signals will bring their contribution as some of them will be transmitted at the same frequencies as the GPS signals. However, if affected by radio frequency interference, a receiver can lose one or more frequencies leading to the use of only one frequency to estimate ionospheric code delay. Therefore, it is felt by the authors as an important task to investigate the performance of techniques trying to sustain multi-frequency performance when a multi-constellation receiver installed in an aircraft loses dual frequency capability, during critical phases of flight.

After a loss of several frequencies leading to a single frequency degraded mode, a receiver can use code and carrier phase pseudoranges made on only one carrier frequency to estimate the ionospheric delay. To achieve this estimation, the receiver can use the difference between code and carrier phase measurements. Indeed, this quantity can be modelled as twice the ionospheric delay plus noise, multipath, and the carrier phase ambiguity. The ionospheric delay can then be extracted from this, provided the ambiguity is properly removed. This can be achieved after convergence of a Kalman

Filter for example, but then cycle slips need to be monitored.

The probability of a cycle slip to occur is low but not negligible for civil aviation purposes. Several causes of cycle slips may be identified. For instance multipath, dynamics, signal blockage and ionospheric scintillation may be sources of this type of rupture in carrier phase measurements. Cycle slips may have random magnitudes. Those ones have to be detected and corrected with a performance compliant with civil aviation requirements for integrity, continuity, accuracy and availability. This problem of cycle slip detection is a priority before analyzing the accuracy of the single frequency iono corrected pseudorange.

We propose to follow the methodology exposed below to assess the performance of potential algorithms of detection (and estimation) of cycle slips. First, the cycle slip detection and correction ability will be defined by the smallest cycle slip detectable with a required probability of missed detection. This smallest detectable cycle slip implies a bias on position error depending on geometry. Therefore, availability of protection against cycle slips compatible with APV 1 and APV 2 for instance, depends on geometry and must be computed at every second.

The main goal of this paper is to know exactly the impact of the capability of cycle slip detection algorithms on the availability of reliable single frequency iono corrected pseudoranges.

I. INTRODUCTION

In case of radiofrequency interference (RFI), the loss of one frequency may be a problem if one wants to keep the same ionospheric correction quality as in the nominal dual frequency case. It would be necessary to use alternate techniques to estimate the ionospheric error in a degraded single frequency case.

Total Electronic Content estimations provided by GPS Klobuchar and Galileo NeQuick models do not provide a sufficient accurate ionospheric delay estimation at any receivers' position (latitude, longitude, altitude, see [NATS, 2003]), for any geometry of satellites in view. Consequently, it is necessary to employ an other technique in a single frequency case.

Code and carrier phase measurements vary differently with ionosphere; they can be jointly used to extract the ionospheric delay. This is the traditional code minus carrier technique [Shau-Shiun Jan, 2003].

Indeed, this difference between code and phase measurements can be modelled as twice the ionospheric delay plus noise, multipath, and the carrier phase ambiguity. The ionospheric delay can then be extracted from this, provided the ambiguity

is properly removed. This can be achieved after convergence of a Kalman Filter for example, but then cycle slips need to be monitored in order not to bias the iono corrected measurement. As the capability of cycle slip detection is not exactly known, our priority is to determine that performance, before analyzing the accuracy of the obtained single frequency iono corrected pseudorange.

Carrier phase measurements are provided by carrier tracking loops. Measurements quality depends on the loop ability to give an approximate value close to the actual value of the carrier phase.

In a nominal case, this loop is able to quickly follow the time evolution of the incoming phase, and measurement errors are small. However, the tracking loop may lose the signal during a short period and then re-acquire it just after the break. Such a phenomenon causes a phase jump (cycle slip) and can be modelled by a rupture, a sudden change from one measurement to the next one. The phase ambiguity will therefore vary in this case. This problem, called cycle slip, occurs when the C/N_0 is low (blockage, multipath) or when the receiver has too important and unpredictable movements. The magnitude of those cycle slips will be a multiple of half the carrier wavelength and multiple of wavelength after half cycle ambiguity resolution through parity check.

Making the difference between code and carrier phase measurements in a single frequency case is therefore a candidate technique for a good estimation of ionospheric error for civil aviation, as mentioned in [NATS, 2003]. In the case where a cycle slip occurs in signal carrier phase, this difference is biased by the magnitude of the cycle slip. We will focus on this code minus carrier divergence technique in the following.

II. KALMAN FILTERING FOR SINGLE FREQUENCY IONOSPHERIC ESTIMATION

The input state of the Kalman filter we mentioned in introduction can take into account the two constellations (GPS and GALILEO) space vehicles. It will estimate both ionospheric delay and ambiguities of all satellites in view [Ouzeau, 2006].

As the convergence time of the filter reaches several tens of seconds (larger than the TTA for our simulations), it is preferable to initialize it in nominal dual frequency mode.

One should take into account the estimation of dynamics parameters as dynamics will have importance in cycle slipping as we will see further in this paper. But, even if those parameters are limited (see GALILEO MOPS, bounded values of acceleration and jerk), additional input state parameters will decrease its robustness, the number of in-view satellites increasing the number of input

states (ambiguities) depending on ambiguity resolution.

The Kalman filter may be hybridized with models, Klobuchar for GPS constellation and NeQuick for Galileo one. Two different approaches may be considered, on the one hand, the use of a unique filter with a state vector composed of ionospheric estimation and ambiguities of all satellites in view from the two constellations. On the other hand, two independent filters may be employed independently considering separately GPS and Galileo constellations. The first approach allows considering a virtual single constellation. The less states in the filter, the more robust the filter will be.

III. CIVIL AVIATION REQUIREMENTS AND CYCLE SLIP DETECTION

In all cases, even in a nominal dual frequency case, cycle slips have an influence on code-carrier smoothing as carrier phase measurements are used to compute smoothed code measurements as described further in this paper. In a single frequency case, with single frequency ionospheric correction, it is particularly important to be able to detect and correct cycle slips. Indeed, code minus carrier divergence seems to be the most interesting technique in case of loss of frequency for civil aviation [NATS, 2003]. The impact of cycle slipping is consequently not negligible as it will be a large source of error in code minus carrier ionospheric estimation, and detection algorithms have to be implemented and tested against civil aviation requirements. For civil aviation, these detection algorithms are important, mostly for critical approaches. ICAO requirements are defined for those phases of flight and are partially recalled further in this paper. These requirements are accuracy, integrity, continuity and availability.

The integrity risk induced by cycle slip detection ability is the product of the probability of occurrence of cycle slips by the probability of missed detection of those jumps in carrier phase measurements.

From integrity and continuity ICAO requirements, cycle slip minimum detectable magnitude is determined computing the probability of cycle slip missed detection and false alarm rate as described in [Ouzeau, 2006]. This methodology and the values used in simulations are recalled in section 5 of this paper.

We focus on the APV phases of flight; we want to determine if the levels of performance required by ICAO can be met with our proposed algorithms described latter.

Indeed, the large sigma values involved when using Klobuchar or NeQuick estimations of ionospheric code delay do not allow supporting flight operations that require vertical protection level computation. We want to know precisely if our proposed code minus carrier plus cycle slip detection technique will allow supporting those operations.

The first phase of flight to consider is consequently APV I. As a consequence, if the results obtained using code minus carrier divergence and cycle slip detection and correction allow satisfying ICAO requirements, the main default of code minus carrier divergence technique will be removed.

The value of the probability of missed detection is deduced from the integrity risk and the probability of occurrence of cycle slips. For APV 1 and APV 2 approaches, the Signal In Space (SIS) integrity risk equals $2*10^{-7}$/approach.

Allowed false alarm probability is determined from continuity ICAO requirements. In [RTCA, 2006], the SIS false alert probability is set to $1.6 \, 10^{-5}$/sample for APV phases of flight.

IV. CYCLE SLIP DETECTION ALGORITHMS PROPOSED

We propose here cycle slip detection algorithms.

There are many possible cycle slip detection techniques. This can be done during data parity check, through a comparison between Doppler-predicted phase and real-time obtained phase, comparison between smoothed and raw pseudoranges and finally, using a generalized likelihood ratio test at the Kalman filter output.

A Kalman filter may estimate ionospheric delay and the ambiguities of all satellites in view, making the difference between code and carrier phase measurements as presented in section II. A Generalized Likelihood Ratio test at the output of this filter can be implemented to detect and estimate cycle slips. It is based on a multiple hypothesis test examining all the possible mean jumps at each instant. A decision is taken comparing the likelihood ratio for the chosen magnitude and time index with a defined threshold. A time-sliding window is used to make the hypothesis test. If a cycle slip rupture is detected, Kalman filter estimations are corrected to take into account the induced error. A computation of cycle slip amplitude is inherent to detection.

We won't describe here the Kalman filter and Generalized Likelihood Ratio in details, the interested reader may find those informations in [Ouzeau, 2006].

We have here mentioned many detection algorithms, other ones may be implemented and a combined use of those algorithms has to be tested.

Detection using predicted phase measurements

This algorithm is based on a prediction of future phase measurements with Doppler measurements:

$$\hat{\phi}(t) = \phi(t - \Delta t) + f_d(t - \Delta t) \times \Delta t$$

Where f_d is the Doppler frequency and Δt is the time delay between the previous and the current measurement.

Then the difference between phase measurements and predicted phase measurements is compared to a threshold which has to be fixed:

$$\left| \hat{\phi}(t) - \phi(t) \right| > Threshold$$

The threshold is a function of false alarm probability with regards to APV phase of flight requirement and on the noise affecting this criterion.

Detection comparing smoothed to raw pseudoranges

Cycle slips on carrier phase measurements will have an impact on the smoothing process. More precisely, code-carrier smoothing is expected to reduce multipath and receiver noise on the pseudoranges and will help us detecting potential cycle slips. Indeed, in this purpose, we compare output and inputs of the smoothing filter described below:

$$P_{proj}(t) = P(t - 1) + (\phi(t) - \phi(t - 1))$$
$$P(t) = \alpha \rho(t) + (1 - \alpha) P_{proj}(t)$$

where:

- P_{proj} is the projected pseudorange in meters
- $P(t)$ is the carrier smoothed pseudo range in meters at time t
- $\phi(t)$ is the accumulated carrier phase measurement in meters at time t
- $\rho(t)$ is the raw pseudo range in meters
- α is the weighting function of the filter, unit less, it is defined by the ratio of the sample time to the smoothing time constant.

The second term of P_{proj} is the difference between two consecutive phase measurements. If a cycle slip occurs at t in the phase measurements, this phase variation will be biased, so the difference between smoothed and raw pseudoranges will abnormally vary.

V. MINIMUM DETECTABLE BIAS

To determine the smallest detectable bias with the required missed detection probability P_{MD}, we launched simulations to determine the performance of some cycle slip detection algorithms.

Different magnitudes of cycle slips must be simulated, and we have to compute non-detection probability and to determine whether the obtained values are acceptable as a function of magnitude of cycle slips.

From ICAO continuity requirements, we tested different cycle slip magnitudes over a sufficient number of samples to reach a required probability of false alarm (1.6 10^{-5}/sample for APV 1). For each cycle slip magnitude, over 1/ (false alarm probability) samples were intentionally biased by that cycle slip and tested with our detection algorithm was tested. A too low number of samples won't provide significant results, as the expected false alarm rate won't be reached with an insufficient number of samples. In principle, the more biased samples are tested, the more significant will be the results. However, we do not dispose of an infinite simulation time. Consequently, simulations were conducted for thirty times the minimum required number of samples (30/false alarm probability).

This provided us a threshold of cycle slip magnitudes.

Then, from integrity requirements ($2*10^{-7}$ per approach for APV) and the cycle slip occurrence probability, we determined the required missed detection probability.

We tested varying cycle slip magnitudes with regards to the obtained threshold over a sufficient number of samples as for false alarm probability (30/missed detection probability), until we reached the required P_{MD}. This provided us the minimum detectable bias with the employed detection algorithm.

This study was made for normal and abnormal aircraft dynamics defined in [MOPS, 2006].

Influence of dynamics

Dynamics of the onboard receiver differs from case to case. Those values are provided by [MOPS, 2006] white paper and are recalled below:

	NORMAL DYNAMICS	ABNORMAL DYNAMICS
Ground speed	**800 Kt**	**800 Kt**
Horizontal acceleration	**0.58 g**	**2.00 g**
Vertical acceleration	**0.5 g**	**1.5 g**
Total jerk	**0.25 g/s**	**0.74 g/s**

Table 1: Normal and abnormal aircraft dynamics, [MOPS, 2006].

Where g = 9.81m/s² and Kt are Knots.

Influence of signal type on detection

The probability of occurrence of cycle slips due to dynamics differs from one signal to another one.

We recall here how we computed this probability for each signal.

We define a flow of events which are cycle slips occurring successively and separated by random time intervals. This process has Poisson characteristics.

So the probability of occurrence during Δt will be:

$$P_{OCC} = \exp(-\overline{T}\Delta t)$$ where $\overline{T}$ is the cycle slip rate and Δt is the exposure time.

$\overline{T}$ is the mean time between two cycle slips.

The cycle slip rate (or cycle slip mean time) is computed using the following formula; see [Holmes, 1990] for a complete demonstration:

$$\overline{T} = \frac{\pi}{2B_L\gamma}\tanh\left(\frac{2\pi\gamma}{\sigma_\phi^2}\right) \times \left[I_0^2\left(\frac{1}{\sigma_\phi^2}\right) + 2\sum_{n=1}^{\infty}(-1)^n \frac{I_n^2\left(\frac{1}{\sigma_\phi^2}\right)}{1+\left(\frac{n\sigma_\phi^2}{\gamma}\right)^2} \right]$$

where I_n are Bessel functions of order n.

σ_ϕ is the phase loop noise, its value depends on the type of loop employed:

- For a Costas loop,

$$\sigma_\phi = \sqrt{\frac{B_L}{\frac{C}{N_0}}\left(1+\frac{1}{2\frac{C}{N_0}T_D}\right)}$$

- For a classical PLL,

$$\sigma_\phi = \sqrt{\frac{B_L}{\frac{C}{N_0}}}$$

where:

- C/N_0 is the carrier to noise density ratio
- T_D is the coherent integration time
- B_L is the loop bandwidth

We can note that this last value of σ_ϕ does not depend on integration time for a classical PLL, but in reality, the integration will play a role for the normalization of the PLL discriminator.

γ represents the constant phase tracking error due to the receiver dynamics (rad). According to [Hegarty, 1997], for a third order PLL, the maximum value of γ is provided by:

$$\gamma_{max} \approx \frac{5.67 j_{max}}{\lambda B_L}$$

where:

- j_{max} is the maximum expected jerk in g/s
- B_L is the loop bandwidth
- λ is the carrier wavelength

For GNSS signals, we first compared the probabilities of occurrence of cycle slips using a Costas loop.

Table 2 summarizes the values obtained:

Signal type	Integration time	Probability of occurrence within 150s
GPS L1 C/A	20 ms	**5.3 e-004**
GPS L5	20 ms	**8.0 e-004**
GALILEO L1	100 ms	**5.3 e-004**
GALILEO E5b	100 ms	**7.7 e-004**

Table 2: Probability of occurrence of cycle slips for each signal within critical phases of fight (150 seconds), during landing. These probabilities are computed considering a Costas PLL, with 10 Hz bandwidth, jerk max of 0.25 g/s (normal manoeuvres), as a function of coherent integration time.

The dependence of these probabilities upon the integration time is negligible (10^{-6} maximum difference on the probability for integration times between 10 ms and 100 ms).

From the required integrity risk, with these probabilities of occurrence, the missed detection probability should be between $24*10^{-4}$ and $4*10^{-4}$ for normal manoeuvres. Finally, to overbound the missed detection probability, the chosen values are

10^{-5} for normal manoeuvres and 10^{-6} for the abnormal manoeuvres case.

Generation of pseudoranges and Doppler measurements for simulations

For the next parts, we generate pseudoranges and Doppler measurements allowing us to control the perturbations affecting signals and dynamics parameters of the receiver.

We generate code, phase and Doppler measurements. Those measurements were generated taking into account dynamics:

$$\Phi(t) = \rho_0 + v \times t + a \times 9.81 \times t^2 + j \times 9.81 \times t^3 + b + multipath + atmosphere + noise$$

$$P(t) = \rho_0 + v \times t + a \times 9.81 \times t^2 + j \times 9.81 \times t^3 + b + multipath + atmosphere + noise$$

where:

- ϕ is the phase measurement in meters

- P is the code pseudo range measurement in meters

- ρ_0 is a typical constant range (ex: 20000 km)

- v is the range rate, taken here to be 800 + 70 m/s (worst case range rate due to satellite and aircraft movement during an approach).

- a is the acceleration in g. It is taken according to table 2 for normal and abnormal maneuvers (further in this paper).

- j is the jerk in g/s. It is taken according to table 2.

- b is the receiver clock bias generated as described in [Winkel, 2000].

The Doppler measurements were generated as a first order derivative of the previously defined phase but the additive noise is provided by Gaussian random values multiplied by a FLL sigma value defined in [Kaplan, 1996] instead of a PLL sigma value:

$$\sigma_{FLL} = \frac{1}{2\pi T_D} \sqrt{\frac{8 W_L}{\frac{C}{N_0}} \left(1 + \frac{1}{T_D \frac{C}{N_0}}\right)} \quad (Hz)$$

The multipath for code measurements is generated by drawing Gaussian random values with a sigma corresponding to the worst case sigma at 5° elevation (for Galileo, this value of mask angle will be 10 degrees) using [SARPs, 2006] formula:

$$\sigma_{multipath} = 0.13 + 0.53 * e^{-\frac{E}{10}} \quad (m)$$

The maximum carrier phase multipath error considered here does not exceed one quarter of a carrier cycle. Indeed, this is the maximum phase tracking error, assuming there is only one signal replica with a magnitude of 1. So the corresponding

chosen sigma value is set to this corresponding "maximum".

The atmospheric effects are generated by multiplying Gaussian random values by a sigma corresponding to troposphere and ionosphere, with an elevation angle E of 5 degrees [Shau-Shiun Jan, 2003].

The sigma for the troposphere is:

$$\sigma_{tropospher\,e} = \frac{0.12 * 0.001}{\sqrt{0.002001 + \sin(E)^2}}$$

The sigma for the ionosphere [Shau-Shiun Jan, 2003]:

$$\sigma_{ionosphere\_phase} = 0.02m$$

$$\sigma_{ionosphere\_code} = 0.83m$$

The error due to noise on the phase and code is generated as random Gaussian values with a sigma corresponding to the standard deviation of the tracking error due to noise.

For phase lock loop, we chose the following value (Costas tracking loop):

$$\sigma_\phi = \sqrt{\frac{B_L}{\frac{C}{N_0}} \left(1 + \frac{1}{2 \frac{C}{N_0} T_D}\right)}$$

where:

- C/N_0 is the carrier to noise density ratio, we chose C/N_0 = 30 dB Hz.

- T_D = 100 ms is the coherent integration time.

- B_L = 10 Hz is the loop bandwidth.

For the delay lock loop, we chose σ_{DLL}=0.4 m.

VI. SIMULATION RESULTS

Smallest detectable cycle slip

In our simulations, using Doppler prediction of phase measurements, the smallest detectable cycle slip has an amplitude of 13 meters for normal dynamics and 16 meters for abnormal maneuvers [Ouzeau, 2006].

The test between smoothed and raw pseudoranges does not provide a better performance of cycle slip detection than Doppler estimations, as the results obtained are a little more than 15.8 meters for normal dynamics and for a window of 100 seconds before the time of estimation.

Those values seem to be high, but this may be explained by the fact we generated pseudo ranges for our tests with worst case sigma values as described in section V of this paper (ionosphere, troposphere, drawing Gaussian random values with sigmas).

Our strategy was first to determine a detection threshold compliant with continuity ICAO requirements and then to determine the smallest detectable bias with regard to integrity requirements.

Since integrity definitions are all in the position domain, we have to switch from the pseudo range variance domain to the position variance domain.

Cycle slip detection availability calculation

Before discussing the accuracy of code minus carrier plus detection algorithm, we choose to represent the availability maps of the Doppler predicted phase detection ability for GPS and Galileo standalone constellations and for the combination of the two. Indeed, if the availability obtained using our proposed algorithms is insufficient for civil aviation, it won't be necessary to discuss the accuracy of estimations. In addition, the Doppler algorithm provided us the best results in detection, that is to say, the smallest minimum detectable bias. That is why we must know if this technique is available enough to meet ICAO requirements.

The smallest detectable cycle slip we will be able to detect will give us an idea of the position error induced by the undetectable error in the single frequency ionospheric corrected range. But this error will depend upon the geometry defined by the positions of the satellites and the receiver. So, we will multiply the bias induced by the inability of our algorithms to detect cycle slips by maximum geometrical factors described latter, in order to compare it with alert limits presented in Table 3, for APV phases of flight.

	HAL	VAL	TTA
APV 1	**40 m**	**50 m**	**10 s**
APV 2	**40 m**	**20 m**	**6 s**

Table 3: Integrity requirements, [MOPS, 2006].

HAL stands for Horizontal Alert Limit, VAL for Vertical Alert Limit and TTA for Time To Alert.

The minimum detectable bias induces an error in code minus carrier (CMC) estimation, and consequently, an error in positioning.

Before discussing the accuracy of our proposed CMC + detection algorithm, we focus on the availability of such a method over Europe.

The bias induced by the capability of the algorithm to detect small cycle slips is introduced in the following equations in order to know precisely the error induced in positioning for a given constellation, considering the worst-positioned satellites.

As described in detail in [Macabiau, 2005], we assume the receiver makes n pseudo range measurements collected in a vector noted Y.

The measurement vector Y and the state vector X composed of positions and clock bias are linked by:

$$Y = g(X) + E$$

E being the measurement error, due to multipath, noise, possible cycle slips, atmospheric effects and satellite clock residuals.

$X = \begin{bmatrix} x & y & z & b \end{bmatrix}^T$ is composed of positions (x, y and z) and clock bias b.

Let us describe the least squares navigation solution of the equation.

If we denote $\hat{X}_0$ an initial estimate of X, we can then note $X = \hat{X}_0 + \Delta X$.

The measurement model can be rewritten as:

$$Y = g(\hat{X}_0 + \Delta X) + E$$

This expression may be linearized around $\hat{X}_0$, the estimate of X:

$$Y \approx g(\hat{X}_0) + \frac{\partial g}{\partial X}(\hat{X}_0).\Delta X + E$$

where:

$$\frac{\partial g}{\partial X}(\hat{X}_0) = G$$

$$= \begin{bmatrix} \frac{\partial g^1}{\partial x}(\hat{X}_0) & \frac{\partial g^1}{\partial y}(\hat{X}_0) & \frac{\partial g^1}{\partial z}(\hat{X}_0) & \frac{\partial g^1}{\partial b}(\hat{X}_0) \\ \vdots & \vdots & \vdots & \vdots \\ \frac{\partial g^n}{\partial x}(\hat{X}_0) & \frac{\partial g^n}{\partial y}(\hat{X}_0) & \frac{\partial g^n}{\partial z}(\hat{X}_0) & \frac{\partial g^n}{\partial b}(\hat{X}_0) \end{bmatrix}$$

We can rewrite the linearized model as:

$$Y - g(\hat{X}_0) = G.\Delta X + E$$

$$\Delta Y = G.\Delta X + E$$

$\Delta Y = Y - g(\hat{X}_0)$ is the deviation between measurements and noiseless predicted measurements if position and clock delay were $\hat{X}_0$.

From this linear relation between ΔY and ΔX, we deduce the least squares estimate of ΔX:

$$\Delta \hat{X} = [G^T G]^{-1} G^T.\Delta Y \quad (1) \text{ and } \hat{X} = \hat{X}_0 + \Delta \hat{X}.$$

The residual ΔY considering $\hat{X}$ may be expressed as:

$$\Delta Y = Y - g(\hat{X}) = g(X) - g(\hat{X}) + E$$

$$\Delta Y = g(\hat{X}_0 + \Delta X) - g(\hat{X}_0 + \Delta \hat{X}) + E$$

As described in [Macabiau, 2005], we linearize the previous expression:

$$Y - g(\hat{X}) \approx G\Delta X - G\Delta \hat{X} + E = G(\Delta X - \Delta \hat{X}) + E \quad (2)$$

however,

$$\Delta \hat{X} = [G^T G]^{-1} G^T [Y - g(\hat{X}_0)],$$

therefore:

$$\Delta \hat{X} = [G^T G]^{-1} G^T [G\Delta X + E],$$

which is equivalent to:

$$\Delta \hat{X} = \Delta X + [G^T G]^{-1} G^T E$$

$$\Delta X - \Delta \hat{X} = -[G^{T}G]^{-1}G^{T}E \qquad (3)$$

Consequently, from (2), we deduce:

$$\Delta Y = Y - g(\hat{X}) = (I - G[G^{T}G]^{-1}G^{T})E$$

and so from (1):

$$\Delta \hat{X} = (G^{T}G)^{-1}G^{T}[I - G(G^{T}G)^{-1}G^{T}]E$$

E contains all the measurement errors and we can note there is a relationship between the measurement error vector E and the prediction error vector ΔY or the least squares estimate of ΔX.

From (3), we deduce the projected errors in horizontal and vertical planes defined by the position of each satellite in view, and in particular, the bias induced by the cycle slip detection algorithm.

The projection for each visible satellite is the linear relationship existing between the estimated horizontal or vertical position error and the pseudo range error to a given satellite. In other words, it is the linear relationship between biases in each of the visible satellites and the induced position error.

These projections are characterized by the geometry matrix G and vary with time; it differs from one satellite to another one.

We note:

$$A = (G^{T}G)^{-1}G^{T}$$

Then:

$$\Delta X - \Delta \hat{X} = -AE$$
$$\hat{X}_{0} + \Delta X - \hat{X}_{0} - \Delta \hat{X} = -AE$$
$$\left\| X - \hat{X} \right\| = \left\| AE \right\|$$

Where $\| \ \|$ is a classical matrix norm.

The difference between X and its estimate is thus described as a function of the measurement error E.

The horizontal and vertical projections of the previous relation are computed using the following equations:

$$\begin{cases} H(i) = \sqrt{A_{1i}^{2} + A_{2i}^{2}} \\ H_{max} = \max_{i}(H(i)) \end{cases}$$

$$\begin{cases} V(i) = A_{3i} \\ V_{max} = \max_{i}(V(i)) \end{cases}$$
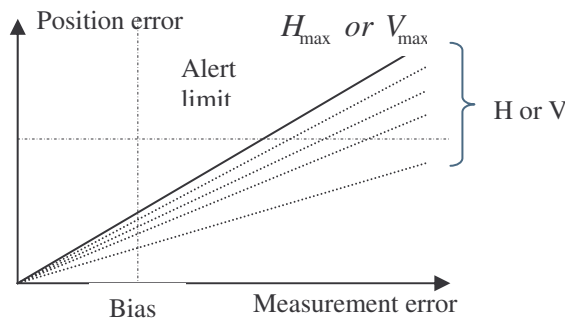
for $i = 1 \ldots n$.

Figure 1: Computed position error for all satellites in view.

As we can see figure 1, the more important the geometrical factor is, the higher the position error is. So we consider the maximum geometrical factor so as to study the worst satellite position case.

The horizontal impact of the undetected bias is thus modeled by:

$$H_{impact} = H_{max} \cdot bias$$

A similar relationship can be used to define the vertical one:

$$V_{impact} = V_{max} \cdot bias$$

H_{max} and V_{max} are the horizontal and vertical projections that induce the maximum position errors in horizontal and vertical planes respectively, considering all satellites in view.

$H_{max}(V_{max})$ is the horizontal (vertical) value of the satellite whose bias is the most difficult to detect.

Note that in the following simulations, we chose to introduce the bias obtained with our Doppler-estimation algorithm.

When the computed impacts (H_{impact}, V_{impact}) are over alert limits (horizontally and vertically), the detection algorithm is declared unavailable. When those impacts are under or equal to alert limits, it is declared available.

Availability maps for GPS and Galileo constellations and aircraft dynamics influence

We focus on APV phase of flight; we draw the availability maps of detection algorithms over Europe independently for normal and abnormal maximum dynamics. Simulations over 24 hours for GPS and over 10 days for Galileo, show that using GPS or Galileo constellations in standalone mode, the availability of cycle slip Fault Detection function is far from being sufficient for normal aircraft dynamics when using only detection using Doppler measurements. It is also consequently the case for abnormal dynamics; we only represent here a normal maneuver case for each constellation since as we can see, the availability requirement is not fulfilled for standalone modes.
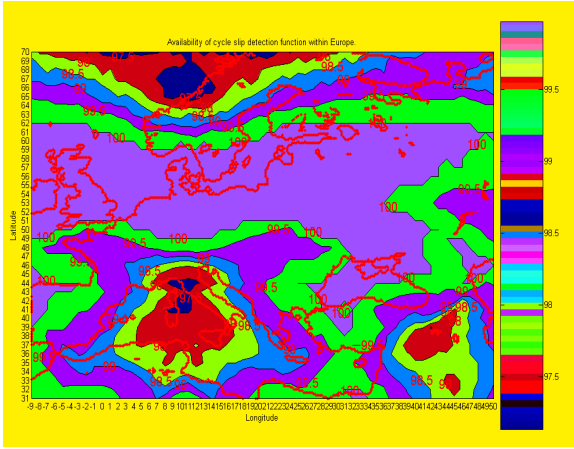
1303

Figure 2: Availability of proposed cycle slip detection algorithm over Europe considering GPS constellation only and normal aircraft dynamics, for APV 1 alert limits.
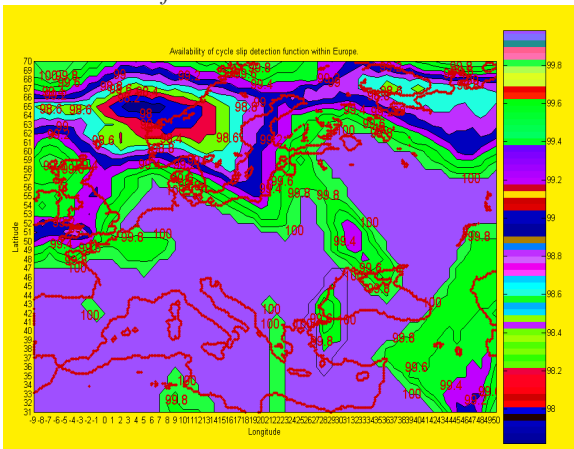

Figure 3: Availability of proposed cycle slip detection algorithm over Europe considering Galileo constellation only and normal aircraft dynamics for APV 1 alert limits.

As we can see in figure 2, for GPS, assuming normal dynamics, a maximum value of 100% availability is reached but only in Northern Europe. The minimum value obtained is 97.1%. The mean value is 99.5%. This is felt as not sufficient for aviation purposes. This means that single frequency GPS measurements corrected from ionospheric delay through CMC technique plus cycle slip detection can not be used in standalone mode, as the minimum required continuity value during APV I phases of flight is 99.99%.

As seen in figure 3, for Galileo constellation, assuming normal dynamics, the results obtained show that availability is sufficient over a large part of Europe but not enough over Norway for instance. The minimum availability is 97.8%, the mean value is 99.63% and the maximum is 100%. Cycle slip risk in single frequency iono corrected measurements is consequently also not covered by Galileo in a standalone mode for APV I.

Note that, this lack of availability for GPS and GALILEO single frequency ionospheric correction plus cycle slip detection is mainly due to the largest impact of the bias on the vertical error. This is due to the fact that the geometrical factor $(G^T G)^{-1} G^T$ is larger on the vertical axis than on the horizontal plane.

Recall that the bias included in the availability computation is calculated for the higher value of dynamics. That is to say the availability is calculated for maximum jerks and accelerations of an aircraft in a normal dynamics case. We thus considered the least favorable case for each calculation of availability.

However, when combining GALILEO and GPS constellations, as we can expect, the availability map shows a considerable improvement of the availability (100% over Europe for both APV 1 and APV 2, for normal and abnormal manoeuvres). As we are in the particular case of a single frequency mode, this dual constellation case will occur when only one frequency is available for both GPS and Galileo constellations. However, the combined use of GPS and Galileo induces failure modes which are still badly analyzed. This combined mode must be considered with simplified hypothesis.

Therefore, if we want to use one of the standalone constellations, the detection algorithm would have to be improved so as to keep the continuity of the single frequency code minus carrier divergence technique.

VII. CONCLUSION AND PERSPECTIVES

The objectives of this paper were to know if our proposed single frequency CMC and detection algorithms allow maintaining the dual frequency performances during APV. Because the analyzed CMC technique is sensitive to cycle slips, we first focused on the cycle slip detection capability. We therefore analyzed the availability of the detection method over Europe for GPS and Galileo constellations for all kinds of aircraft dynamics.

From our simulations, it is shown that the minimum detectable bias induced by cycle slip detection algorithms does not allow to support flight operations that require vertical protection level computation (APV), using one of the two constellations (GPS or Galileo) in standalone mode. This is represented by the plotted availability maps over Europe (97.8% minimum availability for Galileo and 97.11% for GPS constellation in standalone mode). When combined, the availability obtained is 100% for normal and abnormal aircraft dynamics.

However, further investigations have to take into account the potential integrity problems due to

the combined use of GPS and Galileo constellations.

We have analysed the availability of the proposed detection techniques, following the integrity and continuity ICAO requirements. Now the accuracy of the proposed algorithms could be discussed regards to civil aviation requirements.
Also, after detection, a reparation algorithm may be employed. The magnitude estimation of cycle slips may be provided by a Generalized Likelihood Ratio algorithm as mentioned in [Ouzeau, 2006].

Another point to underline is the hybridization of a Kalman filter with Klobuchar or NeQuick models to perform the estimation of ionospheric delay. This hybridization will depend upon the considered constellation.

One of the questions after discussing the single frequency estimation is how to bridge gaps between nominal dual frequency mode and degraded single frequency mode. One of the responses to bring to this question is the use of a Kalman filter run with dual frequency measurements in the nominal mode, and used in the degraded mode with single frequency measurements only.

REFERENCES

[Bastide, 2002] Note on Acquisition, Tracking and Demodulation Thresholds Computation Spectrum Subgroup meeting, Washington DC, USA, April 8th – 12th, 2002, Frederic Bastide, Benoît Roturier.

[Hegarty, 1993] Hegarty Christopher J., "An Assessment of Alternative Methods of Mitigating Ionospheric Errors for WADGPS Users", MITRE Technical Report MTR93W111, The MITRE Corporation, McLean, Virginia, 1993.

[Hegarty, 1997] Christopher Hegarty: Analytical Derivation of Maximum Tolerable In-Band Interference Levels for Aviation Applications of GNSS, Navigation, The Journal of the ION, Vol 44, N° 1, Spring 1997.

[Holmes, 1990] Coherent Spread Spectrum Systems, Robert E. Krieger Publishing Company, Malabar, Florida, Holmes, 1990.

[Kalman, 1993] Kalman Filtering, Theory and Practice, Mohinder S.Grewal, Angus P. Andrews, Prentice Hall Information and System Sciences Series, Thomas Kailath, Series Editor.

[Kaplan, 1996] Understanding GPS, Principles And Applications, Elliott D. Kaplan, Artech House, Boston, London, 1996.

[Lestarquit, 1995] Determination of the Ionosphere Error Using Only L1 Frequency GPS Receiver, Laurent Lestarquit, Norbert Suard, Jean-Luc Issler, CNES, 1995.

[Macabiau, 2005] RAIM Performance in Presence of Multiple Range Failures, C. Macabiau, B. Gerfault, I. Nikiforov, L. Fillatre, B. Roturier, E. Chatre, M. Raimondi, A-C. Escher, ION National Technical Meeting 2005.

[MOPS, 2006] Interim Minimum Operational Performance Specification For Airborne Galileo Satellite Receiving Equipment, White Paper, EUROCAE, May 2006.

[NATS, 2003] Sustainable Mobility and Intermodality Promoting Competitive and Sustainable Growth, Maintaining Dual Frequency Navigation Performance in the Presence of Interference, 2003.

[Nisner, 1995] GPS Ionosphere Determination Using L1 Only, Paul Nisner, UK National Air Traffic Services, Mike Trethewey, Signal Computing Ltd, ION 1995.

[Ouzeau, 2006] Ionospheric Code Delay Estimation in a Single Frequency Case for Civil Aviation, proceedings of the ION GNSS, Fort Worth, 2006.

[RTCA, 2006] Radio Technical Commission for Aeronautics, do229c, 2006.

[SARPs, 2006] Standards and Recommended Practices, ICAO, 2006.

[Shau-Shiun Jan, 2003] Aircraft Landing Using a Modernized Global Positioning System And The Wide Area Augmentation System, Shau-Shiun Jan, May 2003.

[Willsky, 1976] A.S. Willsky and H. L. Jones (1976). A generalized likelihood ratio approach to the detection and estimation of jumps in linear systems. IEEE Trans. Aut. Control, 21, pp. 108-112.

[Winkel, 2000] PhD Thesis dissertation, 2000.